

Tensor product random matrix theory

Alexander Altland

Institut für Theoretische Physik, Universität zu Köln, Zùlpicher Str. 77, 50937 Cologne, Germany

Joaquim Telles de Miranda and Tobias Micklitz

Centro Brasileiro de Pesquisas Físicas, Rua Xavier Sigaud 150, 22290-180, Rio de Janeiro, Brazil

(Dated: November 1, 2024)

The evolution of complex correlated quantum systems such as random circuit networks is governed by the dynamical buildup of both entanglement and entropy. We here introduce a real-time field theory approach — essentially a fusion of the $G\Sigma$ functional of the SYK model and the field theory of disordered systems — engineered to microscopically describe the full range of such crossover dynamics: from initial product states to a maximum entropy ergodic state. To showcase this approach in the simplest nontrivial setting, we consider a tensor product of coupled random matrices, and compare to exact diagonalization.

Introduction:—When addressing the physics of complex many-body systems, an early choice needs to be made: One option is to focus on individually resolved quasiparticle trajectories, which in concrete terms means working with second quantized representations, many-body field integrals, and related concepts. The alternative is to consider the more complex trajectory of the system at large, as described by a single exponentially high-dimensional Hamiltonian matrix. Depending on the context, the preferred choice is usually evident, use cases including large portfolio of many-body field theory approaches to condensed matter systems, or the modeling of complex nuclei in terms of high dimensional random matrix theories, respectively. However, since the advent of synthetic quantum matter, we are increasingly witnessing applications in twilight zones, where the appropriate approach is not so clear. For example, starting from initial product states of qudits or quasiparticles, circuit dynamics addresses the buildup of complexity, eventually leading to a fully entangled state. In the latter, individual states can no longer be meaningfully resolved and global representations, e.g., in terms of a high-dimensional random matrices, may be more appropriate. The crux of the matter is that precisely the crossover dynamics leading from individually resolved quasiparticle world lines to the single complex trajectory of a many-body state is hard to capture in terms of the analytical toolkits of field or path integration, which may be a reason for the relative scarcity of such methods in the theory of quantum circuits. (For powerful phenomenological, semiclassical, or statistical mechanics inspired approaches, see, e.g., Refs. [1–7].)

In this paper we define a random matrix model displaying such type of crossover dynamics in the simplest possible setting. The model will serve as a test bed for a path integral approach whose central ingredient is an interaction vertex possessing the mathematical structure of a Hadamard product. We will discuss how the Hadamard vertex catalyzes the progressive locking of initially separate subsystem trajectories to a configuration representing a maximally entangled ergodic final state. As a representative of various observables witnessing this dynamics we will consider the spectral form factor, whose time dependence we will compute ana-

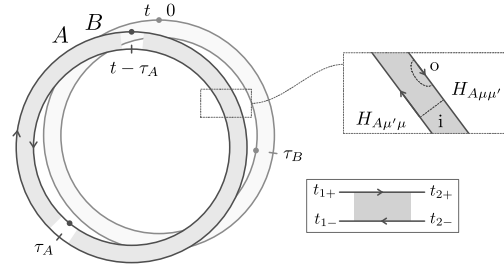


Figure 1. Schematic representation of closed scattering sequences in A and B Hilbert space traversed in retarded and advanced time order (outer and inner rings), and starting and ending at times 0 and t , respectively. For constructive interference, the sequences must contain the same scatterers but can be traversed at a relative time delay, τ_A and τ_B , indicated by dots on the retarded and advanced contours. Insets: In- and out-scattering induced by H_A , and temporal structure of the Gaussian propagator Eq. (3).

lytically and compare to exact diagonalization. We conclude with a discussion of the extensibility of the approach exemplified here to more complex circuit arrays.

The model comprises two N_X -dimensional qudits, $X = A, B$, governed by the Hamiltonians $H_A \otimes \mathbb{1}_B$ and $\mathbb{1}_A \otimes H_B$, with H_X drawn from a Gaussian random matrix ensemble. The two sectors are entangled via the likewise random $N_A N_B$ -dimensional Hamiltonian H_{AB} , defining the full Hamiltonian $H = H_A + H_B + H_{AB}$, where we suppress trivial factors $\otimes \mathbb{1}$ for notational simplicity. Floquet variants of this model have been recently studied with a focus on spectra [8, 9], eigenstates [10], and entanglement properties [10–13]. While these analyses were based on combinations of semiclassical, perturbative, and numerical approaches, we here aim for a first-principles analysis of the Hamiltonian system by field integral methods.

We begin our analysis of this model with a qualitative discussion in terms of Feynman path amplitudes. This picture will provide an intuitive basis for the subsequent quantitative formulation in terms of a real-time matrix path integral.

Qualitative discussion: In the absence of coupling, the

spectrum of our model comprises all $N_A N_B$ different sums $\epsilon_{A_i} + \epsilon_{B_j}$. While these levels can come arbitrarily close (no RMT-like level repulsion) they remain statistically correlated (no Poisson statistics). To understand these correlations, it is best to switch to time space, and consider the spectral form factor, which, prior to normalization, is defined as $K(t) = \langle \text{tr}(G^+(t))\text{tr}(G^-(-t)) \rangle$ in terms of the retarded and advanced Green's functions $G^\pm(t) = \mp i\Theta(\pm t)\exp(-iHt)$. Consider first a single ergodic system, such as the A factor of our tensor product structure. Representing the trace as $\text{tr}(\dots) = \sum_\mu \langle \mu | \dots | \mu \rangle$, the form factor becomes a double sum over self-returning scattering paths traversed in time t , as indicated in Fig. 1. To leading approximation in N_A^{-1} , only paths traversing the same sequence of scattering events in retarded and advanced chronology contribute upon averaging over the ensemble. However, the anchor points at which the sequences start in Hilbert space at time $t = 0$ can be independently chosen for the two amplitudes, and it is this sliding degree of freedom which is responsible for the linearity $K(t) \sim t$ [14]. Turning to the full problem, the trace assumes the form $\text{tr}(\dots) = \sum_{\mu\nu} \langle \mu\nu | \dots | \mu\nu \rangle$, where we use the shorthand notation $\langle \mu\nu | \equiv \langle \mu | \otimes \langle \nu |$, and the second factor labels the states of B . On this basis, we now compare the two alternative approaches mentioned above, paraphrased as second vs. first quantized for brevity.

Second quantized: Consider the states $|\mu\nu\rangle = a_\mu^\dagger b_\nu^\dagger |0\rangle$ represented in terms of single-particle bosonic operators generating the subsystem states. Beginning with the uncoupled system, $H_{AB} = 0$, the factorization of the trace $\text{tr}(G^\pm(t)) = \text{tr}(G_A^\pm(t))\text{tr}(G_B^\pm(t))$ is manifest in this language. It extends to the form factor, and so $K(t) \sim t^2$ in this limit. However, upon switching on the interaction, we encounter the *nonlinear* operator (summation convention) $H_{AB} = a_\mu^\dagger b_\nu^\dagger H_{\mu\nu,\mu'\nu'} a_{\mu'} b_{\nu'}$, expected to send the full system into an ergodic regime. Defining the variances of our random Hamiltonians as $N_A \langle |H_{A\mu\mu'}|^2 \rangle = N_B \langle |H_{B\nu\nu'}|^2 \rangle = \lambda^2$, and $N_A N_B \langle |H_{AB\mu\nu,\mu'\nu'}|^2 \rangle = \Lambda^2$, a straightforward Golden Rule estimate suggests a coupling rate $\gamma \propto \Lambda^2/\lambda$, and hence we expect $K(t) \sim t$ for time scales $t > \gamma^{-1}$. However, the quantitative description of this crossover requires the solution of an interacting problem, which is non-trivial in this language.

First quantized: In this representation, $H_{\mu\nu,\mu'\nu'}$ is a matrix of dimension $N_A N_B$, and the derivation of a linear form factor $K(t) \sim t$ follows standard protocols (for example, by interpreting the construction indicated in Fig. 1 in terms of scattering paths in tensor product space.) However, it is no longer straightforward to describe the crossover to $K(t) \sim t^2$ upon *lowering* Λ ; extracting the disentangling into separate subsystem paths in μ and ν space and the emergence of two independent sliding symmetries from the global matrix representation is difficult. We observe that neither approach appears to be well suited to address the middle ground between the two limiting regimes.

Field integral approach: In the following, we follow a

strategy inspired in equal parts by field theories of disordered systems [15], and the $G\Sigma$ approach to the SYK model (for a review, see Ref. [16]), to construct a theory tailored to describe the form factor at all time scales. Referring to the Supplemental Material for details [17], we start in second quantization and next turn to a real-time field integral representation, $K(t) = \langle \prod_{s=+,-} a_{\mu,t}^s b_{\nu,t}^s \bar{a}_{\mu,0}^s \bar{b}_{\nu,0}^s \rangle$, where $a = \{a_{\mu,t}^s\}$ and $b = \{b_{\nu,t}^s\}$ are now complex commuting field variables, and the causal index ($s = \pm$) distinguishes between fields propagating forward and backward in time. The functional average $\langle \dots \rangle = \int D(a, b) \exp(iS[a, b]) (\dots)$ is over the action $S[a, b] = S_0[a, b] + S_{\text{int}}[a, b]$, with $S_0[a, b] = \int_0^t dt \sum_{x=a,b} \bar{x} \tau_3 (i\partial_t - H_X + i0\tau_3)x$, and $S_{\text{int}}[a, b] = \int dt \bar{a} \bar{b} \tau_3 H_{AB} ab$, where Hilbert space indices are suppressed for clarity, and τ_3 is a Pauli matrix in contour space. The (Itô) time discretization of the functional integral implies $\langle 1 \rangle = 1$, i.e. it yields real-time Green's functions without the need for explicit normalization [18].

Averaging over the distribution of the three involved random matrices produces an effective action containing products of up to eight field operators. They all occur in combinations summed over Hilbert space indices, suggesting the introduction of effective Hubbard-Stratonovich variables $(G_X)_{tt'}^{ss'} \equiv -iN_X^{-1} x_{\mu,t}^s \bar{x}_{\mu,t'}^{s'} (-)^{s'}$. We effect this locking via Lagrange multipliers $(\Sigma_X)_{tt'}^{ss'}$, and arrive at the representation $\langle \dots \rangle = \int D(G, \Sigma) \exp(iS[G, \Sigma])$, where $S = S_A + S_B + S_{AB}$, with

$$S_X[G, \Sigma] = iN_X \text{tr} \left(\ln(i\partial_t - \Sigma_X) + G_X \Sigma_X + \frac{\lambda^2}{2} G_X^2 \right),$$

$$S_{AB}[G] = i \frac{\Lambda^2 N_A N_B}{2} \text{tr}((G_A \odot G_B \tau_3)^2). \quad (1)$$

Here, the traces imply summation over all indices, $\text{tr}(AB) = \int dt dt' A_{tt'}^{ss'} B_{t't}^{s's}$, and we encounter the Hadamard or element-wise product defined as $(A \odot B)_{tt'}^{ss'} = A_{tt'}^{ss'} B_{tt'}^{ss'}$. In the same notation, the correlation function assumes the form $K(t) = (N_A N_B)^2 \langle (G_A \odot G_B)_{t,0}^{++} (G_A \odot G_B)_{0,t}^{--} \rangle$.

Stationary phase: The introduction of the collective (G, Σ) variables is rewarded by the appearance of the factors N_X upfront the action, inviting a stationary phase approach. For simplicity, we assume that the coupling H_{AB} is sufficiently weak to not significantly affect the mean-field Green's functions of our system. Temporarily neglecting the Hadamard vertex, a variation of the action in G and Σ (we suppress the label $X = A, B$ for readability) then leads to the equations $G = (i\partial_t - \Sigma)^{-1}$ and $\Sigma = \lambda^2 G$, which are solved by $\bar{G}_{tt'} = -i\tau_3 \Theta(\tau_3(t - t')) \exp(-\lambda|t - t'|)$: the average Green's functions and the self-energies are rapidly decaying functions in time, respecting causality. Neglecting ∂_t in comparison to Σ , the saddle point equations are approximately invariant under temporally slow rotations, $\bar{G} \rightarrow T \bar{G} T^{-1}$, $T = \{T_{tt'}^{ss'}\}$. (Note that the rotational symmetry breaking in causal space, $\bar{G} \propto \tau_3$, identifies the T 's as Goldstone mode fluctuations, with ∂_t an 'explicit symmetry breaking'.) The expansion of the action to leading order in

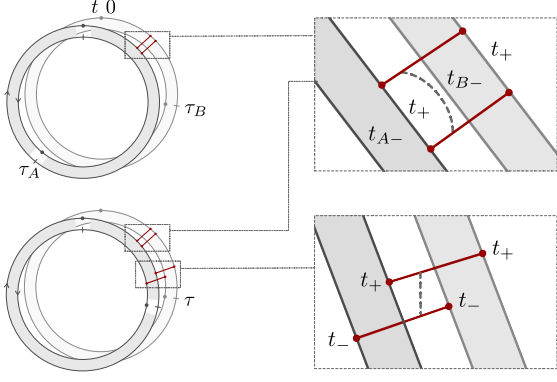


Figure 2. Correlation function in the presence of interactions. Top: For scattering path traversing Fock space in generic, asynchronous order, only the two-body generalization of out-scattering or self-energy damping is operational. Bottom: for time-synchronized path, or equal-time scattering sequences in tensor space, in-scattering cancels against out-scattering, stabilizing an undamped ergodic model.

derivatives ∂_t reads as $S[T_A, T_B] = \sum_X S_{\rho_X}[T_X]$, where

$$S_{\rho}[T] = i\pi\rho \int dt dt' \text{tr}(\tau_3 T_{tt'}^{-1} (\partial_{t'} + \partial_t) T_{t't}), \quad (2)$$

is the real-time representation of the matrix actions known to produce the random matrix form factor of systems with spectral density $\rho_X = N_X/(\pi\lambda)$ [15, 19]. With the notation $Q = T\tau_3 T^{-1}$, our correlation function assumes the form $K(t) = \rho_A^2 \rho_B^2 \prod_X \langle Q_{Xt,0}^{++} Q_{X0,t}^{--} \rangle$, the factorization implying that at this level we obtain the product form factor of the decoupled theory.

However, what is not so evident is how for finite Λ the Hadamard coupling vertex will result in a collapse to a single Goldstone mode Q required to describe an emerging ergodic phase. Naively, one might speculate that its proportionality to $G_A \odot G_B \sim Q_A \odot Q_B$ enforces a locking $Q_A = Q_B = Q$ of the fluctuation fields. However, this is not how it works. It is straightforward to verify that the vertex does not vanish on such field configurations, implying that sought-after modes must be realized differently. The crossover problem articulated in the beginning now assumes a very concrete form: our path integral must possess a single Goldstone mode with a uniquely specified action. However, it is not obvious where this mode hides.

Perturbation theory: In order to get traction with this problem, and establish contact to the above Feynman path picture, we turn to a more concrete level and expand the Goldstone mode fluctuations in generators chosen to anti-commute with the saddle point $\sim \tau_3$, $T = \exp(B\tau_+ - B^\dagger\tau_-)$, where $\tau^\pm = \frac{1}{2}(\tau_1 \pm i\tau_2)$ and $B = \{B_{tt'}\}$ [19]. The quadratic expansion of the decoupled theories assumes the form $S[B] = 2i\pi\rho \int dt dt' B_{tt'} (\partial_t + \partial_{t'}) B_{t't}^\dagger$, implying that the Wick contraction of matrices in this free

quadratic theory is given by

$$\langle B_{t_1+t_1-} B_{t_2-t_2+}^\dagger \rangle = \Delta\delta(\Delta t_1 - \Delta t_2)\Theta(t_2 - t_1), \quad (3)$$

with $\Delta = 1/(2\pi\rho)$, $\Delta t = t_+ - t_-$ and $t = (t_+ + t_-)/2$, and the δ function broadened on the minimal timescale resolved by the B theory, λ^{-1} . Physically, these modes describe the pair propagation of states indicated in the lower inset of Fig. 1, where the temporal constraints imply equal propagation time of the retarded and advanced amplitude, $t_{2+} - t_{1+} = t_{2-} - t_{1-}$, and causality $t_{2s} > t_{1s}$. Otherwise, the B propagator is structureless, reflecting ergodicity. Substitution of the expansion $G_{t,0}^{++} \rightarrow \text{const.} + \int d\tau B_{t,\tau} B_{\tau,0}^\dagger$ and application of the contraction yields each of the correlation functions as a product of two modes (Fig. 1), leading to $K(t) = \prod_X \left(\rho_X^2 \int_0^t d\tau_X \cdot 1 \right) \propto t^2$, i.e. the product of two form factors, individually proportional to t . The influence of the Hadamard vertex becomes transparent once we subject it, too, to the generator expansion. Referring to the Supplemental Material [17], the latter starts at fourth order, $S_{AB} = S_{o+} + S_{o-} + S_i$ with

$$S_{o+}[B] = c_o \int dt_+ \prod_X \int dt_X B_{Xt_+t_X} B_{Xt_X-t_+}^\dagger, \quad (4)$$

$$S_i[B] = -c_i \int dt_+ dt_- B_{At_+t_-} B_{Bt_+t_-} B_{At_-t_+}^\dagger B_{Bt_-t_+}^\dagger,$$

indicating that (a) we are expanding around a proper saddle point and (b) it does not induce a trivial mass as a quadratic term would. Here, $c_o = 2iN_A N_B \Lambda^2 / \lambda^3$, $c_i = 16iN_A N_B \Lambda^2 / \lambda^4$, and the action S_{o-} is obtained from S_{o+} by an exchange $B \leftrightarrow B^\dagger$. These expressions describe the two-body analogs of the elementary one-body self-energy and vertex, o and i indicated in the inset of Fig. 1. Specifically, $S_{o,\pm}$ represents a damping term correlating the previously independent pair amplitudes in A and B Hilbert space through 'out-' scattering processes, cf. Fig. 2 top (for the discussion of a similar damping mechanism for SYK-like models or coupled circuits, cf. Refs.[1, 6, 7]). Coupling only to retarded ($A+, B+$), respectively, advanced ($A-, B-$) amplitudes, it leaves the time differences $\tau_A = t_{A+} - t_{A-}$ and $\tau_B = t_{B+} - t_{B-}$ unconstrained. By contrast, the competing (note the opposite sign) 'in-' scattering vertex does couple advanced and retarded amplitudes, where the instantaneous of the scattering between the A and B sector requires $\tau_A = \tau_B$, cf. Fig. 2, bottom.

Including these vertices into the computation of the correlation function, we obtain the situation depicted in Fig. 2. Prior to interactions (cf. Fig. 1), the correlation function $K(t)$ implies the independent integration over two time arguments τ_X , $X = A, B$, parametrizing the temporal delay between retarded and advanced scattering paths. Upon switching on interactions, generic of these amplitudes suffer out-scattering (top figure), and hence get exponentially damped. However, for synchronous paths $\tau_A \approx \tau_B \equiv \tau$ in-scattering balances the out-scattering and an undamped

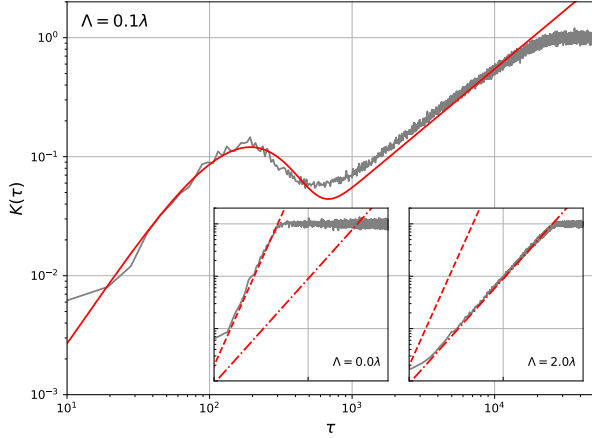


Figure 3. Comparison of the spectral form factor Eq. (5) (red) and numerical simulations (gray), for $\Lambda/\lambda = 0, 0.1$ and 2. Dashed and dash-dotted lines in the insets indicate quadratic, respectively, linear profiles. For the main plot we use three fitting parameters, resulting in good agreement (see main text for further discussion).

contribution ensues (bottom figure). The integral over the single parameter τ then produces the proportionality $K(t) \sim t$ indicative of ergodicity. The projection onto synchronous paths implies that we are effectively summing over trajectories in tensor product space $t \mapsto |\mu\nu\rangle(t)$, rather than over products of single-particle trajectories $t \mapsto |\mu(t)\rangle$ and $t \mapsto |\nu(t)\rangle$.

A straightforward summation over interaction vertex insertions of arbitrary order leads to the result

$$K(t) = \frac{c}{N_A N_B} ((t\delta)^2 e^{-2\gamma t} + t\delta), \quad (5)$$

where $\gamma \approx \Lambda^2/(2\lambda)$, the coupling rate, $\delta \sim \lambda$ is set by the width of the spectrum, and c a numerical factor of order $\mathcal{O}(1)$. The first and second term in Eq. (5) are the exponentially damped contribution of generic asynchronous pairs of single-qudit paths, and that of undamped tensor product trajectories, respectively. Our findings are in agreement with the recent results [8] for the spectral form factor in a related Floquet model, and the chaotic regime of a complex SYK model [7].

Numerical validation: Before discussing how the analysis above can be pushed beyond the level of perturbation theory, let us discuss how it fares in comparison to numerics. Fig. 3 shows the analytical prediction Eq. (5) and exact diagonalization results obtained by sampling over 500 realizations of the matrix model with dimensions $N_A = N_B = 130$. The comparison involves three fit parameters, $(a, b, c) = (1.08, 0.44, 2.11)$ defined through the proportionalities, $\gamma = a\Lambda^2/2\lambda$, $\delta = b\lambda$, and the normalization in Eq. (5), respectively. The reason why the values a, b are left unspecified is that our definition of the form factor effectively integrates over all states in the spectrum, whereas

the analytical calculation is based on approximations valid in the band center. While we have not been ambitious to push the computation to the higher level of refinement required for a parameter-free comparison, the nonmonotonous profile of the form factor predicted by Eq. (5) at intermediate values of the coupling is quantitatively confirmed [20].

Generalizations: It is straightforward to generalize the above construction beyond perturbation theory, and in this way identify the Goldstone mode action governing the system in the long time limit: Starting from the matrix representation of observables as $\psi_{At}\psi_{Bt}\psi_{A't'}\psi_{B't'}\dots \rightarrow (Q_{A\tau_3} \odot Q_{B\tau_3})_{tt'}\dots$, we imagine each of the constituent Goldstone modes expanded in generators $W = B\tau_+ - B^\dagger\tau_-$, leading to expressions like $(W_A^n \odot W_B^n)_{tt'}$ at n th order in the expansion. We now observe that each individual Wick contraction applied in the reduction of such expansions must be subject to the equal-time difference condition, $W_{At,t+\tau_A}W_{Bt,t+\tau_B} \rightarrow W_{At,t+\tau}W_{Bt,t+\tau} = (W_A \odot W_B)_{t,t+\tau}$, to escape the damping by out-terms. The recursive application of this condition, implies the collapse $(W_A^n \odot W_B^n)_{tt'} \rightarrow ((W_A \odot W_B)^n)_{tt'}$. Finally, the individual generators appearing in this Hadamard product must be contracted subject to the rule Eq. (3). With Eq. (3), and the idempotency $\Theta^2(t-t') = \Theta(t-t')$, we find that the product of A and B contractions is equivalent to a single one, $W_A \odot W_B \rightarrow W$, governed by the action Eq. (2), where $Q = T\tau_3 T^{-1}$ and $T = \exp(W)$, with the two-body density of states $\rho \propto N_A N_B$. In this way, we demonstrate how at time scales exceeding the coupling time, $t \sim \lambda/\Lambda^2$ the effective theory of an ergodic regime in a Hilbert space of dimension $N_A N_B$ emerges.

Summary and discussion: We have constructed a path integral describing the evolution of a tensor product of two weakly coupled random qudits. For times shorter than a Golden Rule coupling time, the latter evolve as nearly independent, but individually ergodic subsystems, subject to weak damping due to the interqudit relaxation. However, a crucial feature of the integral is that it selects temporally synchronous paths which are exempt of damping and eventually combine to define the ergodic phase of the coupled system. Alongside the semiclassical picture, these contributions afford a nonperturbative description in terms of a Goldstone mode, Q , representing the universal causal symmetry breaking principle indicative of ergodic quantum chaos. Turning back to the tension between first and second quantization raised in the beginning, we note that had we approached the problem in the former that Goldstone mode would have been visible from the beginning [15]. However, in this formulation the opposite short time regime, requiring the emergence of two independent modes representing the subsystems looks inaccessible (or at least we have not managed to describe it within this framework.)

The exploration of a minimal problem prompts considerations regarding the extensibility to more intricate cases, such as systems in the SYK class, where the challenge of bridging between short time quasiparticle evolution [16] and

long time ergodicity [21] remains unresolved, or networks of coupled circuits. While these must be considered on a case-by-case basis, a few overarching observations can be made. First, interacting models subject to statistically independent random coefficients generically lead to path integrals with Hadamard vertices. (A case in point is the $G\Sigma$ -action of the SYK model, which is governed by an operator $G^{\odot 4}$ in the notation of the present paper.) Second, we have seen that the emergence of a universal ergodic Goldstone mode via this operator followed from a cancellation of self-energy (out) and vertex (in) scattering processes, which in turn is a robust feature of unitarity. On this basis, we are optimistic that the concepts introduced here, will become instrumental in the analytical description of more complex use cases of entanglement dynamics.

Acknowledgements:— A.A. acknowledges partial support from the Deutsche Forschungsgemeinschaft (DFG) through the Cluster of Excellence Matter and Light for Quantum Computing (ML4Q) EXC 2004/1 390534769 and the CRC network TR 183 (project grant 277101999) as part of project A03. TM acknowledges financial support by Brazilian agencies CNPq and FAPERJ, and J.T.M. financial support by Brazilian agency CAPES. **Data and materials availability:** Processed data and python script used to generate Fig. 3 are available in Zenodo with identifier 10.5281/zenodo.10949792 [22].

-
- [1] A. Chan, A. De Luca, and J. T. Chalker, Spectral statistics in spatially extended chaotic quantum many-body systems, *Phys. Rev. Lett.* **121**, 060601 (2018).
- [2] A. Nahum, J. Ruhman, S. Vijay, and J. Haah, Quantum entanglement growth under random unitary dynamics, *Physical Review X* **7**, 031016 (2017), publisher: American Physical Society.
- [3] R. Vasseur, A. C. Potter, Y.-Z. You, and A. W. W. Ludwig, Entanglement transitions from holographic random tensor networks, *Physical Review B* **100**, 134203 (2019), publisher: American Physical Society.
- [4] S. Roy, J. T. Chalker, and D. E. Logan, Percolation in fock space as a proxy for many-body localization, *Physical Review B* **99**, 104206 (2019), publisher: American Physical Society.
- [5] A. Chan, A. De Luca, and J. T. Chalker, Solution of a minimal model for many-body quantum chaos, *Phys. Rev. X* **8**, 041019 (2018).
- [6] S. J. Garratt and J. T. Chalker, Local pairing of feynman histories in many-body floquet models, *Phys. Rev. X* **11**, 021051 (2021).
- [7] Y. Liao and V. Galitski, Universal dephasing mechanism of many-body quantum chaos, *Physical Review Research* **4**, L012037 (2022), publisher: American Physical Society.
- [8] F. Fritzsche and M. F. I. Kieler, Universal spectral correlations in interacting chaotic few-body quantum systems, *Phys. Rev. E* **109**, 014202 (2024).
- [9] S. C. L. Srivastava, S. Tomsovic, A. Lakshminarayan, R. Ketzmerick, and A. Bäcker, Universal scaling of spectral fluctuation transitions for interacting chaotic systems,

Phys. Rev. Lett. **116**, 054101 (2016).

- [10] A. Lakshminarayan, S. C. L. Srivastava, R. Ketzmerick, A. Bäcker, and S. Tomsovic, Entanglement and localization transitions in eigenstates of interacting chaotic systems, *Phys. Rev. E* **94**, 010205 (2016).
- [11] J. J. Pulikkottil, A. Lakshminarayan, S. C. L. Srivastava, A. Bäcker, and S. Tomsovic, Entanglement production by interaction quenches of quantum chaotic subsystems, *Phys. Rev. E* **101**, 032212 (2020).
- [12] S. Tomsovic, A. Lakshminarayan, S. C. L. Srivastava, and A. Bäcker, Eigenstate entanglement between quantum chaotic subsystems: Universal transitions and power laws in the entanglement spectrum, *Phys. Rev. E* **98**, 032209 (2018).
- [13] T. Herrmann, M. F. I. Kieler, F. Fritzsche, and A. Bäcker, Entanglement in coupled kicked tops with chaotic dynamics, *Phys. Rev. E* **101**, 022221 (2020).
- [14] F. Haake, *Quantum signatures of chaos*, 4th edition (Springer-Verlag, Berlin, 2018).
- [15] K. B. Efetov, *Synergism in Disorder and Chaos* (Cambridge University Press, Cambridge, 1997).
- [16] V. Rosenhaus, An introduction to the SYK model, *Journal of Physics A: Mathematical and Theoretical* **52**, 323001 (2019).
- [17] In the supplemental material we provide details of the real time path integral construction for the tensor product random matrix model.
- [18] A. Kamenev, *Field Theory of Non-Equilibrium Systems* (Cambridge University Press, 2011).
- [19] A. Kamenev and A. Andreev, Electron-electron interactions in disordered metals: Keldysh formalism, *Physical Review B* **60**, 2218 (1999).
- [20] While theory is based on approximations valid in the band center of the random matrix spectrum, the definition of the correlation function $K(t)$ in terms of an unrestricted trace over Green functions implies that the numerical analysis probes energies outside this region. This leads to quantitative uncertainties, which require the introduction of fitting constants.
- [21] A. Altland and D. Bagrets, Quantum ergodicity in the SYK model, *Nuclear Physics B* **930**, 45 (2018).
- [22] A. Altland, J. Telles de Miranda, and T. Micklitz, Data and code for “Tensor product random matrix theory”, 10.5281/zenodo.10949792 (2024).
- [23] A. Altland and B. Simons, *Condensed Matter Field Theory* (Cambridge University Press, 2023).

SUPPLEMENTARY MATERIAL

In this supplemental material we provide details of the real time path integral construction for the tensor product random matrix model.

Real time field integral

We here provide some details of the real time path integral construction of our tensor model. Starting from the second quantized representation of the trace over the time evolution operator, $\text{tr}(G^\pm(t)) = \langle 0 | a_\mu b^\nu \exp(\pm iHt - 0t) a_\mu^\dagger b_\nu^\dagger | 0 \rangle$,

trotterization in terms of a standard bosonic coherent state representation [23], leads to the representation of the correlation function detailed in the main text, where the causal index s distinguishes between the two contour orientations. (For comparison, note that we might just as well have worked with an algebra of creation operators $\{X_{\mu\nu}\}$ as $\text{tr}(G^\pm(t)) = \langle 0|X_{\mu\nu}\exp(\pm iHt - 0t)X_{\mu\nu}^\dagger|0\rangle$, and coherent states associated to these. In this representation, we would have ended up with a Gaussian path integral for the matrix Hamiltonian $H = \{H_{\mu\nu,\mu'\nu'}\}$ (first quantization). However, we have not succeeded to extract the evolution along approximately independent trajectories in A and B space at early times from this representation.)

Doing the Gaussian average over H_A, H_B and H_{AB} , we arrive at a path integral with the action

$$S[\psi] = \sum_{x=a,b} \bar{x}\tau_3(i\partial_t + i0\tau_3)x + \frac{i\lambda^2 N_X}{2} \text{tr}(\Xi_X^2) + \frac{i\lambda^2 N_A N_B}{2} \text{tr}((\Xi_A \odot \Xi_B)\tau_3)^2,$$

where $(\Xi_A)_{tt'}^{ss'} = -iN_A^{-1}a_{\mu,t}^s \bar{a}_{\mu',t'}^{s'}(-)^{s'}$, $(\Xi_B)_{tt'}^{ss'} = -iN_B^{-1}b_{\nu,t}^s \bar{b}_{\nu',t'}^{s'}(-)^{s'}$. Here, the traces include summation over all indices, i.e. $\text{tr}(XY) = \int dt dt' \sum_{ss'} X_{tt'}^{ss'} Y_{t't}^{s's}$, and similarly $\bar{x}Xx \equiv \int dt dt' \bar{x}_t X_{tt'} x_{t'}$. The explicit representation of the Hadamard product reads as $((\Xi_A \odot \Xi_B)\tau_3)_{tt'}^{ss'} = \Xi_{Att'}^{ss'} \Xi_{Btt'}^{ss'}(-)^{s'}$. The dependence of the action on bilinears summed over Hilbert space indices suggests the introduction of collective variables, $\Xi \equiv G$ via a Lagrange multiplier locking: $\delta(\Xi_X - G_X) = \int D\Sigma_X \exp(-\text{tr}(N_X \Sigma_X (G_X - \Xi_X))$. Noting that $\text{tr}(N_X \Sigma_X \Xi_X) = \exp(i\bar{x}\Sigma_X \tau_3 x)$. With the free action given by $\sum_x \bar{x}\tau_3(i\partial_t + i0\tau_3 - \Sigma_X)x$, the Gaussian integration over $x = a, b$ produces the ' $G\Sigma$ ' action (1) in the main text structurally similar to the action describing the SYK model [16].

Stationary phase action

We consider the stationary phase ansatz $\bar{G} \rightarrow T\bar{G}T^{-1} \approx -\frac{i}{\lambda}T\tau_3 T^{-1}$, where we used that, for slowly varying matrices T , $(T\bar{G}T^{-1})_{tt'} = \int dt' T_{tu} \bar{G}_{u-u'} T_{u't'}^{-1} \approx -\frac{i}{\lambda}(T\tau_3 T^{-1})_{tt'} \equiv -\frac{i}{\lambda}Q_{tt'}$, on account of the temporal short-rangedness of \bar{G} . Likewise, $\Sigma = -i\lambda Q$. Entering with this representa-

tion into the action, the quadratic contributions $\text{tr}(G_X^2)$ and $\text{tr}(G\Sigma)$ decouple from the Goldstone modes (because $Q^2 = \mathbb{1}$), while the expansion of the 'tr ln' in ∂_t acting on the Goldstone modes yields

$$iN_X \text{tr} \ln(i\partial_t + i\lambda Q) = iN_X \text{tr} \ln(i\partial_t + i\lambda\tau_3 + iT^{-1}[\partial_t, T]) \approx i\frac{N_X}{\lambda} \text{tr}(\tau_3 T^{-1}[\partial_t, T]).$$

Noting that $N_X/\lambda = \pi\rho_X$ determines the spectral density of the factor systems at the band center, and turning to an explicit integral representation of the trace, we obtain Eq. (2) in the main text.

N_X^{-1} -expansion

The effect of the Hadamard vertex is best studied within in the framework of a perturbative expansion of the Goldstone modes in generators, $T = \exp(W)$, $W = B\tau_+ - B^\dagger\tau_-$, which, in view of the proportionality of the action to N_X is an N_X^{-1} expansion. Considering its structure in causal space, $\text{tr}((G_A \odot G_B)^2) = \sum_{ss'} \text{tr}(G_A \odot G_B)^{ss'}(G_A \odot G_B)^{s's}$, we realize that we get two structurally (and as we discuss in the main text physically) different contribution of lowest, quartic order in B : in the terms $s = s'$ of equal causality we expand one of the two factors $(G_A \odot G_B)^{ss} \rightarrow \bar{G}_A^s \odot \bar{G}_B^s$ to zeroth order in the Goldstone mode generators, and the other to quartic order, e.g., $(G_A \odot G_B)^{ss} \rightarrow -(\lambda_A \lambda_B)^{-1}(B_A B_A^\dagger) \odot (B_B B_B^\dagger)$. We note that the element-wise Hadamard product does not admit other terms at quartic order. Substituting the time representation of \bar{G}_X , we arrive at the first of Eqs. (4) in the main text. Turning to the causality mixing channel, $(G_A \odot G_B)^{+-}(G_A \odot G_B)^{-+s}$, the expansion $G_X^{+-} \rightarrow i\lambda_X B$ and $G_X^{-+} \rightarrow i\lambda_X B^\dagger$ immediately leads to the second line of Eq. (4) in the main text. In the same way, we obtain the Gaussian expansion of the free action stated above Eq. (3) from the Goldstone mode action Eq. (2) in the main text. In the calculation of numerical coefficients of the coupling constants we assume that $B_{t,t'}$ is a slow function in $t+t'$ and independent of $t-t'$, which e.g. gives rise to the Fermi's Golden Rule coupling rate $\gamma \approx \Lambda^2/2\lambda$ approximated by the density of states at energy $\epsilon = 0$. A more accurate calculation accounting for all time-dependencies would rather lead to an energy-averaged density of states, but details are beyond the scope of this work.